Materials Chemistry and Physics 117 (2009) 301–306

Contents lists available at ScienceDirect

Materials Chemistry and Physics

journal homepage: www.elsevier.com/locate/matchemphys

Synthesis of Mo-SBA-1 catalyst via sol–gel process and its activity

S. Wongkasemjit[a,c,*], S. Tamuang[a], W. Tanglumlert[a], T. Imae[b]

[a] The Petroleum and Petrochemical College, Chulalongkorn University, Bangkok 10330, Thailand
[b] Graduate School of Science and Technology, Keio University, Yokohama 223-8522, Japan
[c] Center for Petroleum, Petrochemicals, and Advanced Materials, Chulalongkorn University, Bangkok, Thailand

ARTICLE INFO

Article history:
Received 15 January 2009
Received in revised form 25 May 2009
Accepted 7 June 2009

Keywords:
Sol–gel process
Mesoporous silica
SBA-1
Epoxidation of styrene

ABSTRACT

Mo-SBA-1 was successfully synthesized via sol–gel process using silatrane and molybdenum glycolate precursors as silica and molybdenum sources, respectively, and hexadecyltrimethylammonium bromide (C_{16}TMAB) as template at room temperature. The X-ray diffraction (XRD) result showed the characteristics of a three-dimensional cubic structure, *Pm*3*n* space group. The incorporation of the molybdenum species into the SBA-1 framework was indicated by the diffuse reflectance ultraviolet–visible (DRUV) result, and it was found that 5 mol% of molybdenum could be introduced into the SBA-1 without any extra-framework species. The activity of the synthesized Mo-SBA-1 catalyst was investigated via epoxidation reaction of styrene monomer, and it showed high activity. The only products of this reaction were styrene oxide and benzaldehyde.

1. Introduction

Since the discovery of ordered mesoporous molecular sieve with uniform pore size [1], many researchers have devoted study to its properties and applications. Because of its high surface area, its applications as a catalyst support, adsorbent, host for nanometer-scale quantum object and host structure for nanometer-size guest compounds, are extensively studied [2]. SBA-1 is one of the ordered mesoporous materials possessing three-dimensional cubic structures with space group of *Pm*3*n* [3]. One of the most important properties of SBA-1 is its special pore structure, a 3D channel network or cage-type pore structure with open window, thus introducing a heteroatom, such as titanium, chromium, vanadium, and molybdenum, onto silica framework is possible [4–7]. Therefore, development of the SBA-1 mesoporous molecular sieve material in the field of catalysis is of much interest.

Huo et al. [8] and Kim and Ryoo [9] synthesized SBA-1 via a direct method using tetraethylorthosilicate [TEOS] as a silica source and a cetyltriethylammonium bromide (C_{16}TEABr), template with a large head group, in highly acidic conditions at low temperature. On the other hand, Tunglumlert et al. [10] synthesized SBA-1 via sol–gel process using silatrane precursor, directly prepared from fumed silica, in the dilute acidic condition at room temperature. Either the direct method or the sol–gel process provides the formation of SBA-1 via $S^+X^-I^+$ mechanism, where S, X and I stand for surfactant, halide and inorganic species, respectively [8–10].

Among various metal atoms that can be introduced into SBA-1, molybdenum, normally used as a catalyst in many organic reactions because of its high catalysis activity and stability, is chosen in this study. Although Mo-SBA-1 had been synthesized by Dai et al. [7] and Che et al. [11], using the synthesized cetyltriethylammonium bromide (C_{16}TEABr) template at low temperature (0 °C), this work was undertaken to synthesize Mo-SBA-1, using a simple template at room temperature, and also focused on both incorporation of Mo species into SBA-1 and the activity of the synthesized materials. The synthesis of Mo-SBA-1 was studied via sol–gel process, using silatrane, molybdenum glycolate precursors, which can be simply produced. Cetyltrimethylammonium bromide (C_{16}TMAB), the commercial surfactant was used as template. The synthesis procedure was carried out at room temperature. The synthesized catalysts were characterized using various techniques, such as XRD, TEM, DRUV, surface area and average pore size analyzer, and SEM. Additionally, the activity of the synthesized Mo-SBA-1 catalyst was investigated via epoxidation reaction of styrene monomer, H_2O_2 oxidant, reaction time and temperature, amount of catalyst and amount of Mo loaded are the factors studied. Products of the epoxidation reaction were analyzed using gas chromatography (GC). The conversion of styrene is calculated on the basis of the amount of styrene monomer used.

* Corresponding author at: The Petroleum and Petrochemical College, Chulalongkorn University, Bangkok 10330, Thailand. Tel.: +66 2 218 4133; fax: +66 2 215 4459.
E-mail address: dsujitra@chula.ac.th (S. Wongkasemjit).

0254-0584/$ – see front matter © 2009 Elsevier B.V. All rights reserved.
doi:10.1016/j.matchemphys.2009.06.004

2. Methodology

2.1. Materials

Fumed silica (SiO_2, 99.8%) and cetyltrimethylammonium bromide (C_{16}TMAB) from Sigma–Aldrich; triethanolamine (TEA) from Carlo Erba; ethylene glycol (EG) from J.T. Baker, USA; sodium sulfate from Ajax Finechem; molybdenum (VI) oxide from Fluka; acetonitrile, sulfuric acid, sodium hydroxide, hydrogen peroxide, and styrene nomomer from Labscan, Asia, were all used as received.

2.2. Preparation of silatrane precursor

The synthesis of silatrane followed the procedure reported in Ref. [12], by mixing SiO_2 and TEA in a simple distillation set using EG as solvent. Reaction occurred at the boiling point of EG under N_2 atmosphere and continued for 10 h, followed by removing EG under vacuum to obtain crude solid product. The crude product was purified by washing with acetonitrile to obtain highly pure silatrane.

2.3. Preparation of molybdenum glycolate

Molybdenum glycolate was synthesized, following the procedure described in Ref. [13], by mixing MoO_3 and EG with vigorous stirring and heating at the boiling point of EG under N_2 atmosphere for 15 min. The obtained solution was centrifuged to separate the unreacted MoO_3. The solution part was left at room temperature for 3 days to obtain molybdenum glycolate solid, followed by washing with acetonitrile and drying in a dessicator.

2.4. Synthesis of mesoporous SBA-1 [10]

Solution A was first prepared by adding C_{16}TMAB to 30 ml of water and stirred for 30 min to obtain a clear solution. Solution B was prepared by adding 5 mmol silatrane and 1.7 mmol NaOH to 14 ml of 0.3 M H_2SO_4, and stirred for 30 min to obtain a homogeneous solution. Solution B was then added to Solution A under vigorous stirring, followed by continuous stirring for 4 h. The mixture was then centrifuged to separate the unreacted materials. The obtained solution was aged at room temperature for 3 days to form precipitate. The product was filtered and washed with distilled water. The pure and dry product was finally calcined at 560 °C using a Carbolite Furnace (CFS 1200) with a heating rate of 0.5 °C min^{-1} to remove template.

2.5. Synthesis of Mo-SBA-1

Solutions A and B were prepared in a method similar to the synthesis of SBA-1; after adding solution B to solution A, molybdenum glycolate precursor was added to the mixture. The mixture was stirred for 4 h, followed by centrifuging to separate the unreacted materials. The obtained solution was aged for 3 days to obtain crude product. The crude product was filtered and washed with distilled water to obtain white solid, followed by calcining at 560 °C to result in Mo-SBA-1. To compare with the Mo-SBA-1 synthesized by the sol–gel process, Mo-SBA-1 was also prepared by wetness impregnation method by dropping molybdenum glycolate solution onto SBA-1, followed by oven drying at 100 °C and calcination at 560 °C.

2.6. Activity study of Mo-SBA-1

Epoxidation reaction of styrene was carried out by using a batch-type reactor [14]. Catalyst (x g), styrene monomer (10 mmol), an H_2O_2 oxidant (9.8 mmol, 30 wt% aqueous solution) and the solvent acetonitrile (10 ml) were added into a glass flask. The factors studied were amount of catalyst used, reaction time, reaction temperature, and amount of Mo loaded. After the catalyst was filtered, the reaction mixture was analyzed by GC to observe the reactants and the products. The conversion of the styrene was calculated on the basis of the amount of styrene used.

3. Results and discussion

Pure SBA-1 and Mo-SBA-1 synthesized via the sol–gel process and calcined at 560 °C gave the XRD patterns shown in Fig. 1. All of the samples showed three well-resolved XRD diffraction peaks at 2θ of 2.2°, 2.4°, and 2.6°, which are indexed to the {2 0 0}, {2 1 0}, and {2 1 1} reflections, respectively. These diffraction peaks are characteristic of the cubic *Pm*3*n* space group [3] and are the same as those of pure silica SBA-1 [8]. In addition, some weak peaks in the range of 3.5–6° indicate that the calcined sample has a high order cubic mesostructure, as described by Che et al. in 2001 [11]. However, the decrease of intensity of the {2 0 0} and {2 1 1} reflections with increasing molybdenum content in the silica framework suggests that the structure of Mo-SBA-1 containing higher molybdenum content is less ordered than that of Mo-SBA-1 having lower content. Since the Mo–O bond length is longer than Si–O, the decrease in the {2 1 0} reflection of Mo-SBA-1, compared to that of its pure SBA-1, could confirm the incorporation of the molybdenum into SBA-1 framework [15].

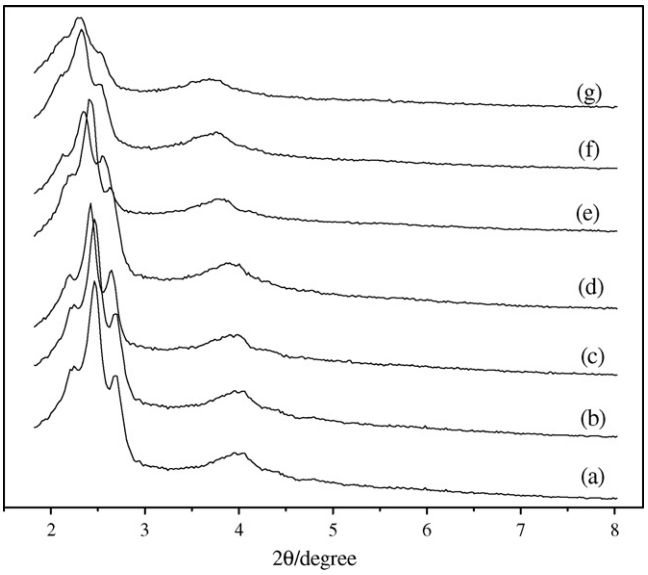

Fig. 1. XRD patterns of the calcined SBA-1 samples containing: (a) pure SBA-1, (b) 0.70, (c) 1.43, (d) 3.5, (e) 5.00, (f) 7.20, and (g) 10.0% Mo.

Transmission electron micrographs (Fig. 2) showed well aligned channel, confirming the long range well-ordered cubic structure of the synthesized materials. A diffuse reflectance UV–vis (DR-UV) spectrometer is used to determine local molecular coordination sphere and bonding information for inorganic compounds. The results are shown in Fig. 3. According to Cotton and Wilkinson in 1980 [16], ligand–metal charge transfer of oxomolybdenum compounds (O^{2-}–Mo^{6+}) caused the adsorption band in the UV–vis region, and the position of this electronic transition depends on the ligand field symmetry surrounding the Mo center. The tetrahedral $Mo^{6+}(T_d)$ is expected to show a higher energy transition than the octahedral one [17]. The band at 230 nm is the characteristic peak of MoO^{4-} species due to the transition of an oxygen 2pπ electron into the empty d-orbital of molybdenum, as also found in Jezlorowski

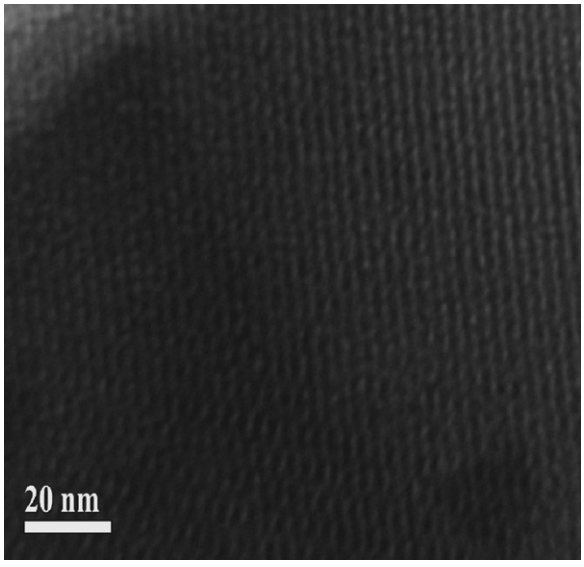

Fig. 2. TEM image of the Mo-SBA-1 samples containing 7.38% Mo.

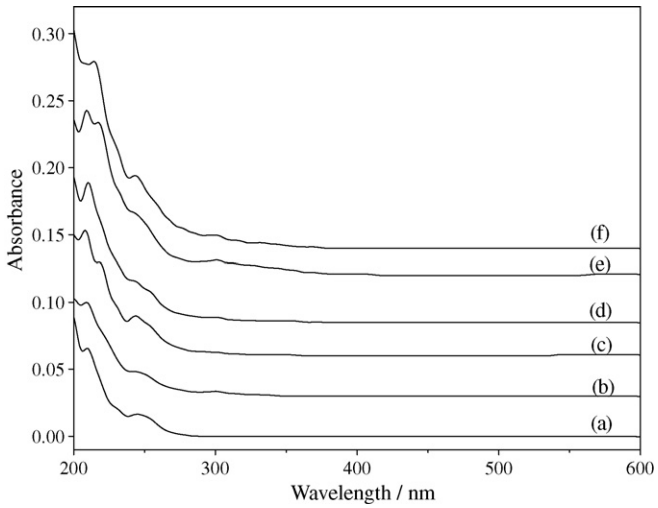

Fig. 3. DRUV spectra of the calcined SBA-1 samples containing: (a) 0.70, (b) 1.43, (c) 3.5, (d) 5.00, (e) 7.20, and (f) 10.0% Mo.

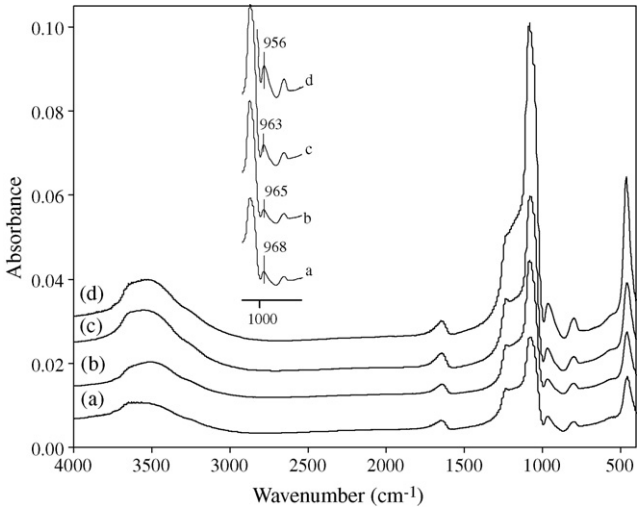

Fig. 4. FTIR spectra of the synthesized Mo-SBA-1 materials: (a) pure SBA-1, (b) 0.70, (c) 1.43, and (d) 5.00% Mo.

and Knözinger's work in 1979 [18]. Che et al. also indicated that the 230 nm band provided the indication of the MoO^{4-} species incorporated in the silica framework via the Mo–O–Si bridge [11]. The band at 250 nm corresponds to Mo^{6+} (T_d). Characteristic of MoO_3, the octahedral Mo^{6+} species (O_h (t_{2u},$t_{1g} \rightarrow t_{2g}$)), is indicated by the band at 320 nm [11]. Therefore, the disappearance of the peak at 320 nm suggests the lack of MoO_3 ($Mo^{6+}(O_h)$). It is likely that most of the Mo were incorporated in the silica SBA-1 framework [11] and had tetrahedral coordination as indicated by the band at 250 nm. From Fig. 3, it is also found that 5% molybdenum can be introduced into an SBA-1 framework without any extra-framework.

The functional group of the synthesized Mo-SBA-1 samples was investigated using FTIR shown in Fig. 4. Generally, the broad band around 3500 cm^{-1} and the peak around 1640 cm^{-1} are the O–H stretching of Si–OH and the bending of physisorbed water. The strong peaks at 1080 and 800 cm^{-1} are the asymmetric and symmetric stretching of Si–O–Si, directly related to the silica framework [19]. The band at 456 cm^{-1} corresponds to Si–O bending [20]. Furthermore, a band at 968 cm^{-1} also indicates the asymmetric stretching of Si–O–Si of SBA-1, which is shifted to 963 cm^{-1} for the Mo-SBA-1 samples. The peak intensity increased with the amount of molybdenum content. According to Morey et al. [21], this asymmetric stretching of Si–O–Si could be shifted to a lower position when one silica atom is replaced with a heavier atom, implying that the molybdenum species were incorporated into silica framework.

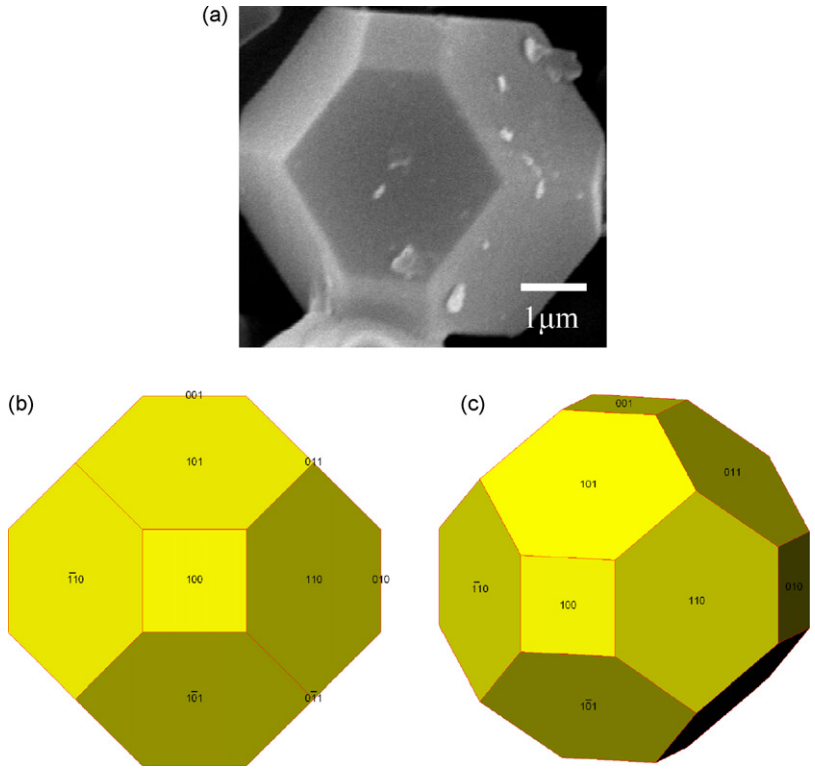

Fig. 5. (a) SEM image of the synthesized SBA-1, (b) and (c) the models of the SBA-1 particle with the plane index.

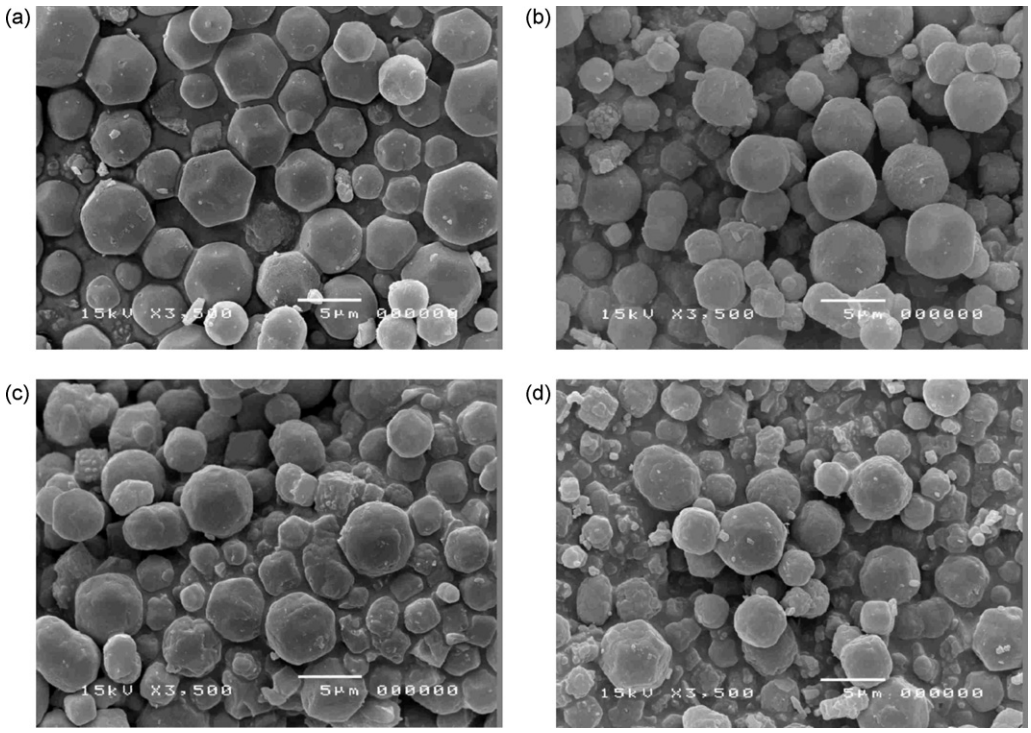

Fig. 6. SEM images of the calcined Mo-SBA-1 samples containing: (a) 1.43, (b) 3.50, (c) 5.00, and (d) 7.20% Mo.

The scanning electron micrograph of the synthesized pure SBA-1 is shown in Fig. 5a–c. The clear crystal-like external morphology of an octadecahedron (18 hedron) with 6 square {1 0 0} and 12 hexagonal {1 1 0} planes is consistent with the cubic structure observed by Guan et al. in 2000 [22], and Lin and Mou in 2002 [23]. When molybdenum species were incorporated into the silica framework of SBA-1, the octadecahedron surface exhibited a more isotropic morphology, as shown in Fig. 6. According to the surfactant–silica assembly mechanism proposed by Hou et al. in 1994 [8], the formation of cubic *Pm*3*n* mesophase occurs through a $S^+X^-I^+$ pathway under acidic conditions and the final product is dependent on the components of the reaction system. The difference in the surface morphology of pure SBA-1 and Mo-SBA-1 was considered in the difference of their inorganic (I^+) species concentration. In addition, the higher amount of the molybdenum results in a greater difficulty of cubic *Pm*3*n* formation, and more isotropic morphology was observed.

N_2 adsorption/desorption isotherms and their corresponding pore size distribution curves obtained from the desorption branch of the calcined Mo-SBA-1 samples containing various contents of Mo are presented in Fig. 7. All samples exhibit isotherms of type IV adsorption isotherms, which is a typical characteristic of mesoporous solids [24]. The sharp inflection at a relative pressure of $P/P_0 = 0.1–0.3$ corresponds to capillary condensation within the uniform mesopores. The Mo-SBA-1 showed a very narrow pore size distribution with a pore diameter of about 21 Å, indicating that the structure of these materials was uniform (Fig. 8). In addition, all samples showed a high surface area (>1000 $m^2\ g^{-1}$). The incorporation of molybdenum into the SBA-1 has a significant effect on the

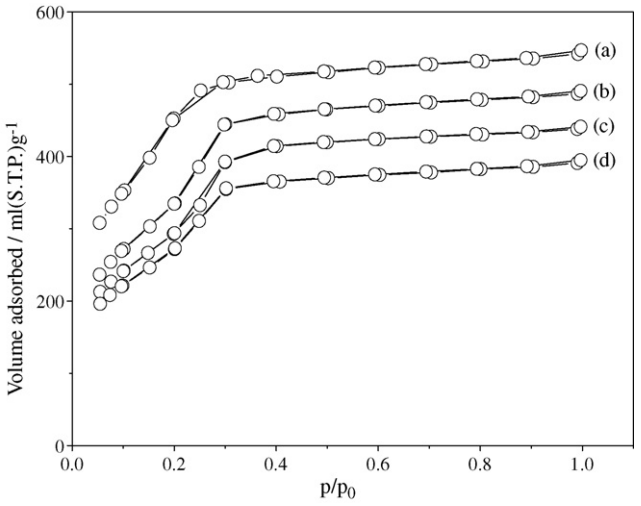

Fig. 7. Nitrogen adsorption/desorption isotherms of the calcined SBA-1 samples containing (a) 1.43, (b) 3.50, (c) 5.00, and (d) 7.20% Mo.

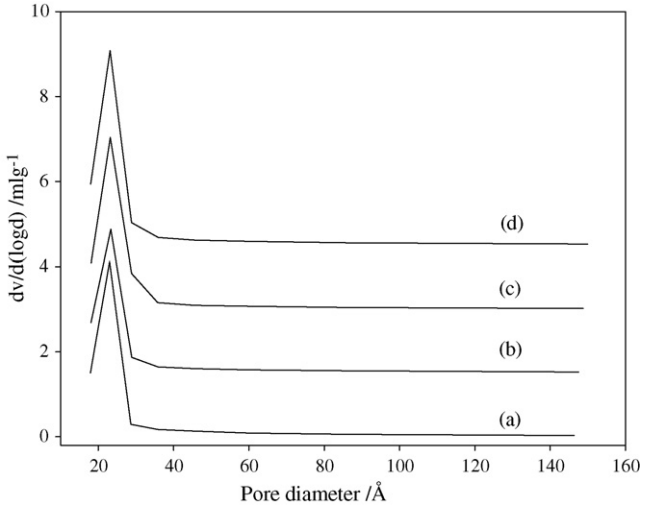

Fig. 8. Pore size distributions of the calcined SBA-1 samples containing (a) 1.43, (b) 3.50, (c) 5.00, and (d) 7.20% Mo.

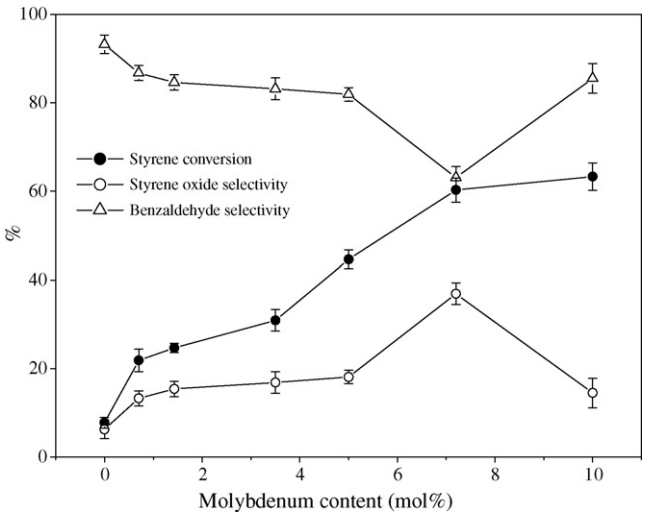

Fig. 9. Effect of the molybdenum content on epoxidation of styrene carried out at 70 °C reaction temperature for 3 h with 0.1 g catalyst.

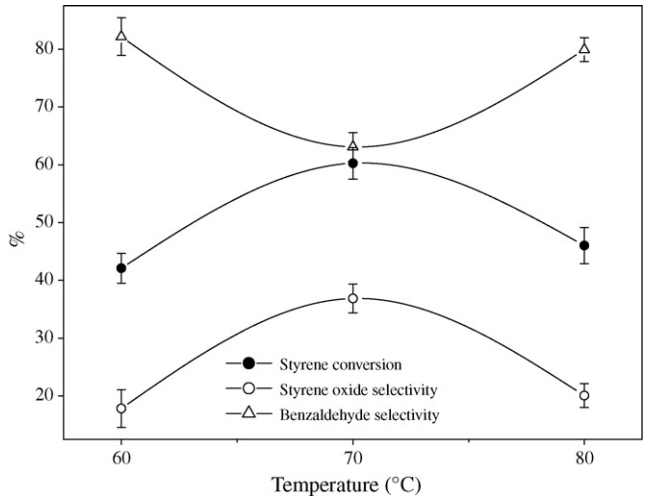

Fig. 10. Effect of the reaction temperature on epoxidation of styrene using 0.1 g catalyst containing 7.20 mol% Mo for 3 h reaction time.

specific surface area of the materials. With increasing molybdenum content, the specific surface area and pore volume decreased, as summarized in Table 1, because the silica mesostructure was destroyed by introducing molybdenum species, as also confirmed by the XRD result. High surface areas were observed in our previous studies on SAB-1 syntheses using silatrane precursor [10]. The precursor is more inert toward hydrolysis than TEOS or other commercially available metal alkoxides, thus, a good balance between hydrolysis and condensation reactions was able to achieve, giving enough time for silica molecules to arrange with a high degree of ordering without a collapse of the framework.

3.1. Activity study of Mo-SBA-1

Catalysis activity of the synthesized catalysts was tested via epoxidation reaction of styrene monomer. This reaction was carried out in a batch-type reactor using H_2O_2 as an oxidant. After the reaction was finished and the catalyst was filtered, the obtained products were analyzed by gas chromatography.

As shown in Fig. 9, the only products of the reaction are styrene oxide and benzaldehyde, the latter being the major product. Styrene conversion over pure SBA-1 was relatively low when compared to Mo-SBA-1. The conversion of styrene monomer was strongly dependent on the amount of molybdenum loaded. Conversion increased as the molybdenum content increased from 7.76 ± 1.25 to 63.32 ± 3.07% when the molybdenum content was loaded from 0 to 10 mol%. This increase indicates that not only the molybdenum species in the SBA-1 framework but also the extra-framework species act as the active site for the oxidation reaction. According to the DRUV results, 5 mol% molybdenum loaded is the maximum amount of molybdenum that can be introduced into SBA-1 without extra-framework. It is likely to be concluded that as long as the structure of materials still remain well-ordered, the small amount of extra-framework as in the case of the 7.20 mol% loading, has still improved the activity of the synthesized catalyst. However, when molybdenum content was increased higher than 7.20 and 10.00 mol%, the styrene conversion did not show significant difference due to some collapse in the materials, as indicated in XRD results.

Table 1
Average pore diameters, pore volumes and surface areas of the calcined Mo-SBA-1 samples.

Sample	% Mo loaded	Average pore diameter (Å)	Pore volume ($cm^3\ g^{-1}$)	Surface area ($m^2\ g^{-1}$)
1	0	29.0	0.95	1520
2	2.40	21.35	0.69	1285
3	3.50	22.23	0.68	1219
4	5.30	22.63	0.67	1183
5	7.20	21.72	0.60	1114

It also reveals that the styrene conversion when using 0.70% Mo in SBA-1 is relatively high as compared to Ti-SBA-1 sample containing 0.86% Ti, giving only 10.2% styrene conversion [15]. However, the styrene oxide selectivity was relatively low compared to Ti-SBA-1 sample. The styrene oxide selectivity was also dependent on the amount of the molybdenum content. It reached the highest value, 36.90 ± 2.47%, at 7.20% molybdenum, but decreased to 14.49 ± 3.34% when the molybdenum content was increased to 10.0%. This result could be explained by the loss of the well-ordered pattern in the XRD results. For comparison, molybdenum impregnated into the SBA-1 framework was prepared and its catalytic activity was also studied. The impregnated sample containing 7.0% Mo showed 14.74 ± 1.54% conversion with 9.26 ± 2.87% styrene oxide selectivity. This value is relatively low, as compared to the Mo-SBA-1 containing 7.20% Mo and synthesized via the sol–gel process. Higher dispersion and isolation of molybdenum sites incorporated into SBA-1 via the sol–gel process could be attributed to the enhancement of the catalytic performance in the epoxidation reaction of styrene. This is also consistent with Rana and Viswsanathan [25] who reported that Mo-MCM-41 synthesized by hydrothermal technique showed a higher activity for the oxidation of cyclohexane and gave a more stable cyclohexanol product, in comparison to the impregnated catalyst, due to the presence of tetrahedral coordination molybdenum on silica framework, resulting in the site of the active metal species.

The effect of the reaction temperature was also investigated at three different temperatures in the range of 60–80 °C; see Fig. 10, showing the increase in the styrene conversion from 42.11 ± 2.56 to 60.26 ± 2.72% as the reaction temperature increased from 60 to 70 °C. Further increase of the reaction temperature to 80 °C caused a decrease in styrene conversion to 46.04 ± 3.12% due to the decomposition of H_2O_2 at high temperature [26]. A similar trend was observed with styrene oxide selectivity. The highest styrene oxide selectivity, 36.90 ± 2.47%, was observed when the reaction temperature was at 70 °C, and decreased to 20.08 ± 2.07% at 80 °C while the selectivity of benzaldehyde was increased. This result could be explained by the further oxidation of styrene oxide to benzaldehyde at higher temperature [15].

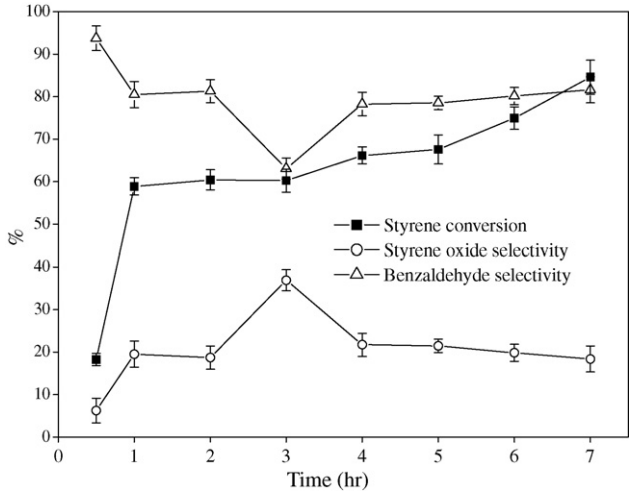

Fig. 11. Effect of the reaction time on the epoxidation of styrene using 0.1 g catalyst containing 7.20 mol% Mo 0.1 g at 70 °C reaction temperature.

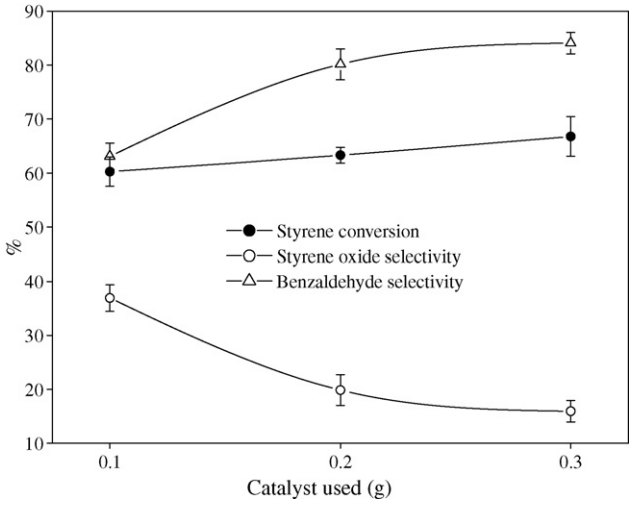

Fig. 12. Effect of the catalyst content on the epoxidation of styrene using 0.1 g catalyst containing 7.20 mol% Mo at 70 °C reaction temperature for 3 h reaction time.

Fig. 11 illustrates the reaction time effect at 70 °C reaction temperature. Expectedly, the styrene conversion increased with the reaction time. The initial reaction was rapid, owing to the full amount of H_2O_2 oxidant [15]. The maximum styrene oxide selectivity, 26.33 ± 1.94%, was reached at 3 h reaction time and slightly decreased with a corresponding increase in benzaldehyde selectivity. This result is consistent with the work of Ji et al., who reported that the formation of benzaldehyde could be attributed to the secondary oxidation of epoxide [15].

The last factor studied was the amount of the catalyst used, as summarized in Fig. 12. Styrene conversion reached 60.26 ± 2.72% when 0.10 g of catalyst was used and did not significantly change when compared with 0.20 and 0.30 g of catalyst. The maximum styrene oxide selectivity was observed at 0.10 g catalyst used. Therefore, the optimum catalyst used was 0.10 g.

4. Conclusions

Mo-SBA-1 was successfully synthesized via the sol–gel process using silatrane precursor as a silica source, C_{16}TMAB as a simple template, and molybdenum glycolate as a molybdenum source, in a dilute acidic condition at room temperature. The obtained materials still maintained a well-ordered mesostructure and high surface area (>1000 $m^2\ g^{-1}$). Optimal amount of molybdenum species loaded into the silica framework without any extra-framework and still maintaining tetrahedral coordination is 5 mol%. In addition, these Mo-SBA-1 materials show relatively high activity in the epoxidation reaction of styrene monomers due to the presence of molybdenum species in an SBA-1 framework. The optimum condition for epoxidation reaction of styrene is at 70 °C reaction temperature for 3 h reaction time using 0.10 g catalyst containing 7.20 mol% of the molybdenum content. The only products obtained from this reaction are styrene oxide and benzaldehyde.

Acknowledgements

The assistance of the following fundings for financial support is deeply appreciated: the Postgraduate Education and Research Programs in Petroleum and Petrochemical Technology (ADB) Fund, Thailand, the Ratchadapisake Sompote Fund, Chulalongkorn University, the Thailand Research Fund (TRF), and the Development and Promotion of Science and Technology Talents Project (DPST), Thailand.

References

[1] C.T. Kresge, M.E. Leonowicz, W.J. Roth, J.C. Vartuli, J.S. Beck, Nature 359 (1992) 710–712.
[2] T.J. Barton, L.M. Bull, W.G. Klemperer, D.A. Loy, B. McEnaney, M. Misono, P.A. Monson, G. Pez, G.W. Scherer, J.C. Vartuli, O.M. Yaghi, Chem. Mater. 11 (1999) 2633–2656.
[3] S. Che, S. Lim, M. Kaneda, H. Yoshitake, O. Terasaki, T. Tatsumi, J. Am. Chem. Soc. 124 (2002) 13962–13963.
[4] D. Ji, T. Ren, L. Yan, J. Suo, Mater. Lett. 57 (2003) 4474–4477.
[5] X. Zhao, X. Wang, J. Mol. Catal. 621 (2007) 225–231.
[6] L.X. Dai, K. Tabaka, E. Suzuki, T. Tatsumi, Chem. Mater. 13 (2001) 208–212.
[7] L.X. Dai, Y.H. Teng, K. Tabata, E. Suzuki, T. Tutsumi, Micropor. Mesopor. Mater. 44–45 (2001) 573–580.
[8] O. Huo, D.I. Margolese, U. Ciesla, D.G. Demuth, P. Feng, T.E. Gier, P. Sieger, A. Firouzi, B.F. Chmelka, F. Schuth, G.D. Stucky, Chem. Mater. 6 (1994) 1176–1191.
[9] M.J. Kim, R. Ryoo, Chem. Mater. 11 (1999) 487–489.
[10] W. Tunglumlert, T. Imae, T.J. White, S. Wongkasemjit, J. Am. Ceram. Soc. 90 (2007) 3992–3997.
[11] S. Che, Y. Sakamoto, H. Yoshitake, O. Terasaki, T. Tatsumi, J. Phys. Chem. B 105 (2001) 10565–10572.
[12] W. Charoenpinijkarn, M. Suwankruhasn, B. Kesapabutr, S. Wongkasemjit, A.M. Jamieson, Eur. Polym. J. 37 (2001) 1441–1448.
[13] S. Sutara, E. Gulari, S. Wongkasemjit, Proceeding of the International Conference on Smart Material (SmartMat-'04), Chiang Mai, Thailand, December 1–3, 2004.
[14] Y. Wang, Q. Zhang, T. Shishido, K. Takehira, J. Catal. 209 (2002) 186–196.
[15] D. Ji, R. Zhao, G. Lv, G. Qian, L. Yan, J. Suo, Appl. Catal. A 281 (2005) 39–45.
[16] F.A. Cotton, G. Wilkinson, Advance Inorganic Chemistry, 4th ed., John Wiley & Sons, New York, 1980.
[17] R.S. Weber, J. Catal. 151 (1995) 470–474.
[18] H. Jezlorowski, H. Knözinger, J. Phys. Chem. 83 (9) (1979) 1166–1173.
[19] D.L. Pavia, G.M. Lampman, G.S. Kriz, Introduction to Spectroscopy, Saunders College Publishing, New York, 1996.
[20] Z. Li, L. Gao, S. Zheng, Mater. Lett. 57 (2003) 4605–4610.
[21] M.S. Morey, J.D. Bryan, S. Schwarz, G.D. Stucky, Chem. Mater. 12 (2000) 3435–3444.
[22] S. Guan, S. Inagaki, T. Ohsuna, O. Terasaki, J. Am. Chem. Soc. 122 (2000) 5660–5661.
[23] H.P. Lin, C.Y. Mou, Acc. Chem. Res. 35 (2002) 927–935.
[24] S. Inagaki, Y. Fukushima, K. Kuroda, K. Kuroda, J. Colloid Interface Sci. 180 (1996) 623–624.
[25] R.K. Rana, B. Viswsanathan, Catal. Lett. 52 (1998) 25–29.
[26] C.V. Rode, U.N. Nethete, M.K. Dongare, Catal. Commun. 4 (2003) 365–369.